



Role of grain boundary and dislocation loop in H blistering in W: A density functional theory assessment

W. Xiao, W.T. Geng*

School of Materials Science & Engineering, University of Science & Technology Beijing, Beijing 100083, China

ARTICLE INFO

Article history:

Received 30 December 2011

Accepted 9 July 2012

Available online 16 July 2012

ABSTRACT

We report a first-principles density functional theory study on the role of grain boundary and dislocation loop in H blistering in W. At low temperature, the $\Sigma 3(111)$ tilt grain boundary can trap up to six H atoms per (1×1) unit in (111) plane before significant sliding occurs. This amount of H weakens greatly the cohesion across the boundary. At room temperature, when only three H can be trapped, this effect can be still significant. A dislocation loop in (100) plane can trap four H per (1×1) unit even at room temperature, whose detrimental effect is strong enough to break the crystal. Our numerical results demonstrate unambiguously the grain boundaries and dislocation loops can serve as precursors of H blistering. In addition, we find no H_2 molecules can be formed in either environment before fracture of W bonds starts, well explaining the H blistering in the absence of voids during non-damaging irradiation.

© 2012 Elsevier B.V. All rights reserved.

1. Introduction

Hydrogen blistering in tungsten, a promising candidate to serve as the plasma-facing material in fusion reactors, has been under intensive study recently [1–3]. A great amount of irradiation experiments have been carried out to shed light on the relationships of retention of H isotopes and the conditions of irradiation (energy, temperature, flux, and fluence) and material preparation (alloying additions, processing, and surface treatment). The blistering in single-crystalline W under non-damaging irradiation is generally believed to occur in association with a very high mobile H concentration as low temperature and long irradiation time are needed, but the precise picture of the spontaneous emission of vacancies in the very initial stage remains elusive [4–7]. In a recent work [8], we show by first-principles density functional theory calculations that when the concentration of H in W exceeds 50%, the formation of both vacancies and self-interstitials becomes exothermic, meaning that spontaneous formation of micro-voids which can accommodate molecular hydrogen will occur. Such a concentration is seemingly unrealistic, but at least it gives the upper limit of the necessary local content of H for blistering to start. By comparison, H blistering in polycrystalline W under high-energy flux is more easily to observe because (i) the pre-existed defects like grain boundaries and dislocation loops can help to build up a high local H concentration by trapping H atoms from the surrounding bulk environment and (ii) the micro-voids formed upon damaging irradiation can even accommodate a small amount H_2 molecules

which can serve as immediate vanguards in gas driven fracture of the crystal lattice [9–11].

The mechanism of H trapping at grain boundaries and dislocations is very similar to what happens at a vacancy, where low-electron-density provides a more comfortable environment for H than interstitial site in perfect lattice [11]. All these traps may act as seeds for bubble growth. Using density functional theory calculations, Liu et al. [12] have demonstrated that at zero temperature a vacancy can trap up to ten H atoms until a H_2 molecule is formed inside the vacancy. Using the same code, Ohsawa et al. [13] have shown that a vacancy can trap up to 12 H atoms and no H_2 molecule can be formed. In almost simultaneous works, Heinola et al. [14] and Johnson and Carter [15], have taken into account the temperature factor, and demonstrated that a vacancy only adsorbs five H atoms at room temperature and no molecules form as expected. For another point defect, substitutional He, Jiang et al.'s work [16] has demonstrated that it can also attract as many as 12 H atoms and no molecules form.

For extended defects like grain boundary (GB) and dislocation loop, the shortest dimension of their free volumes is smaller than that of a vacancy, but the other two dimensions are much larger. Seemingly, we may anticipate these defects being able to accommodate fewer H atoms in the short dimension than in a vacancy, and no H_2 molecule can sit along this direction. However, in the other two directions, i.e., in the grain boundary or dislocation loop plane, it is still possible to position the axes of H_2 molecules. A recent first-principles study by Zhou et al. [17] suggested that the $\Sigma 5(310)$ tilt GB in W can trap no more than two H atoms, and no H_2 molecules can form. They proposed a vacancy trapping mechanism and H bubble could form in GB by adsorbing vacancies. However, the important effects of H on the structure and

* Corresponding author.

E-mail address: geng@ustb.edu.cn (W.T. Geng).

mechanical properties of the GB, i.e. the H induced cleavage along the GB, are still unknown.

To have a detailed knowledge of the local distribution of H near extended defects including grain boundaries and dislocation loops, we have exhaustively examined the segregation (here we neglect the diffusion barrier of H in bulk W, then segregation energy equals trapping energy) of H to two kinds of traps, namely, $\Sigma 3(111)$ tilt GB and a dislocation loop in the (001) plane in W. The $\Sigma 3(111)$ GB has been studied both experimentally [18] and theoretically [19]. The reason we chose a dislocation loop in (100) plane is in view of the reported experimental work in Ref. [6], in which the (100) surface of single crystalline W was electrically polished and irradiated by deuterium for a study of blistering. In addition, to assess the effect of H trapping on the cleavage along the GB or dislocation loop, we have also calculated the adsorption of H on the (100) and (111) planes of W.

2. Computational details

Our DFT calculations were carried out using the Vienna *ab initio* Simulation Package (VASP) [20]. The electron–ion interaction was described using projector augmented wave method [21,22], the exchange correlation potential using the generalized gradient approximation (GGA) in the Perdew–Burke–Ernzerhof form [23]. The lattice constant of bcc W was calculated to be 3.17 Å. For GB systems, we chose a $\Sigma 3(111)$ tilt GB of W using a 29-layer supercell imposing periodic boundary conditions [Fig. 1a]. The slabs were separated by a 10 Å-thick vacuum avoid GB–GB interactions. GB(0) denotes the core of GB, and the other atomic sites are orderly labeled by numbers counted from the GB plane. One unit cell contains two mirror-symmetric 15-layer W atoms arranged at the $\langle 111 \rangle$ direction with one layer in common, which form a tilt GB in between. The thickness of such a cell is large enough to simulate a bulk-like environment in the center of the grain. For dislocation loops, as it could form through the collapse of the vacancy platelets, we removed one layer in a 16-layer supercell to construct a stacking fault. This model is a very simplified one. This is, however,

the only one we can employ because otherwise we have to construct a finite-size dislocation loop immersed in a bulk crystal, which would involve formidable computational effort. As a result, we choose to model a dislocation loop infinitely large. Although the structural information of the edge of such a dislocation loop is unavailable, we are still able to address the effect of free volume supplied by the loop in the core region. Each layer in the supercell has only one atom. The first four layers (two on each side) next to the loop were relaxed and W atoms in other layers were fixed. A $(8 \times 8 \times 2)$ *k*-mesh within Monkhorst–Pack scheme and an energy cutoff of 250 eV were used in both systems. The geometry optimization for each system was continued until the forces on all the atoms were no larger than 10^{-3} eV/Å.

3. Results and discussion

We have evaluated the formation energy of a vacancy at sites from GB(1) to GB(8). It is most stable and exothermic (−0.04 eV) at GB(2), seemingly an indication that the absence of W at GB(2) or GB(−2) is slightly favorable. However, a careful observation tells that it is still an idea $\Sigma 3(111)$ tilt GB after GB(2) is removed, with a decreased slab thickness and a shift of the GB plane from GB(1) to GB(3). The formation energies are 3.66, 2.36, and 3.75 eV at the GB(1), GB(3), GB(4) sites, respectively. At GB(8) it is 3.20 eV, close to the value (3.30 eV) in a perfect bulk environment, a further confirmation that such a supercell is thick enough to model this GB. Though vacancy is undoubtedly another point defect to influence the GB structure and free volume, in this paper we shall only focus on the H role here.

Before implanting H atoms into W, we first optimized the slab thickness [*c* axis in Panel (a) of Fig. 1], and then fixed it when H atoms were added one by one to the pure $\Sigma 3(111)$ tilt GB. For each and every new coming H, we have examined many possible stable configurations, using knowledge gained from previous works [13,16]. The first H prefers to stay close to GB(0) site at the center of the GB core (see Fig. 2). The segregation (trapping) energy, in reference to the H in a perfect bulk interstitial position, is −1.18 eV. And with zero-point energy (ZPE) correction, it is −1.31 eV. For the second and third H, they are respectively −0.99 and −0.80 eV (−1.11 and −0.90 eV with ZPE). The trapped three constitute an equilateral triangle with a side length of 2.02 Å, much larger than H–H bondlength in H_2 (0.75 Å). Segregation of the fourth H becomes much weaker, because the excess volume at the GB has been almost used up, as is evident in Fig. 2. The fourth H incurs a small sliding along the $[11\bar{2}]$ direction, which brings in some more open volume at the boundary and makes the segregation of forthcoming H atoms easier. (The calculated trapping energy for each H is shown in Fig. 3.)

It is very clear from the side view of 7 H system in Fig. 2 that the upper and lower W grains are rather separated along $[\bar{1}10]$, indicating that the segregated H have seriously weakened the cohesion across the boundary. In Fig. 4a, we display the distance between GB(2) and GB(−2) W atoms as a function of the number of trapped H at the GB. For the first six H atoms, it is an approximately linear function; whereas the seventh H atom pushes GB(2) and GB(−2) abruptly up to 3.15 Å, similar to the next nearest neighboring W–W distance. Also, we have calculated the γ -energy of the $\Sigma 3(111)$ GB along $[\bar{1}10]$. It is clearly seen that seven H can greatly reduce the sliding barrier of the GB; and in the most stable configuration the upper and lower W grains experience a relative shift by about 0.2 unit of the $[\bar{1}10]$ Burgers vector. Note that without permission of GB sliding along $[\bar{1}10]$, trapping the seventh H at the GB will not be possible; while without the seventh H, the sliding structure (shown in Fig. 2) would be unstable. In addition, we emphasize that no molecule can be formed at an ideal $\Sigma 3(111)$

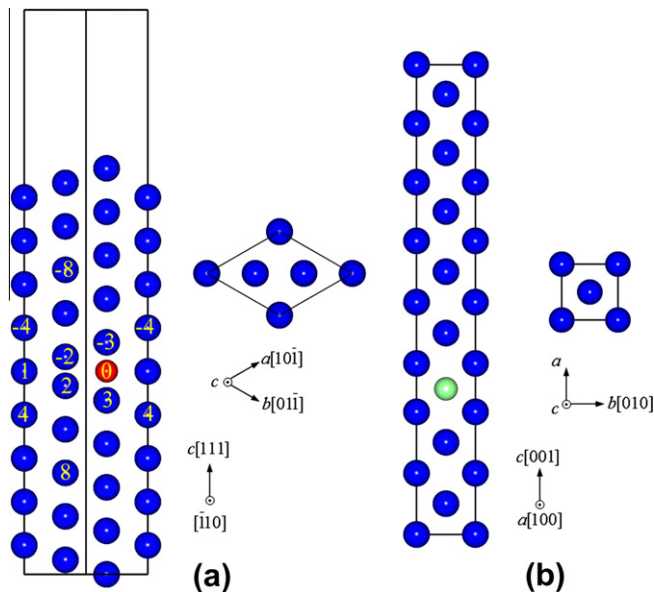


Fig. 1. (a) Side and top views of the computational cell used to model the $\Sigma 3(111)$ tilt GB in bcc W. GB(0) denotes the interstitial site at the GB core. Atoms near the GB are numbered by the atomic layer counted from the GB plane. (b) Model of a dislocation loop in the (100) plane. Light green is the missing layer of W atoms. (For interpretation of the references to colour in this figure legend, the reader is referred to the web version of this article.)

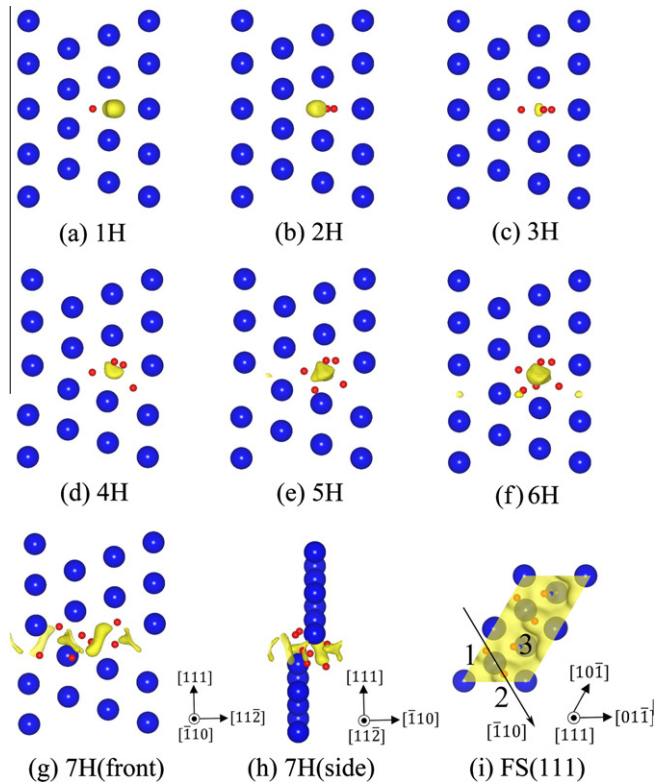


Fig. 2. The calculated geometry and isosurfaces of charge density near a $\Sigma 3(111)$ GB and (111) free surface of W with various number H atoms. Large and blue are W, small and red are H atoms. Yellow curves stand for the charge density isosurfaces of 0.02 e u^{-3} and illustrate the open volume favored by H atoms. In subfigures (a)–(g), the figure is viewed along $[110]$; meanwhile, the side view of 7H system along $[112]$ is also displayed in subfigure (h). For subfigure (i), are listed the order of the adsorbed H on the (111) free surface. (For interpretation of the references to colour in this figure legend, the reader is referred to the web version of this article.)

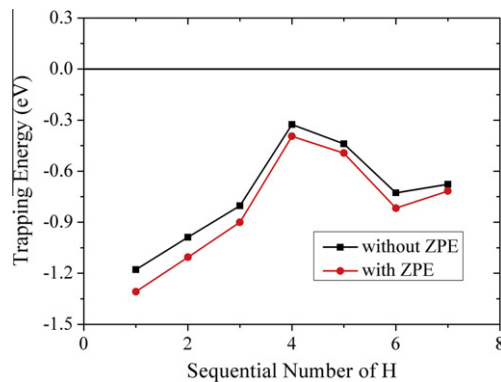


Fig. 3. The calculated trapping energy when one H atom is attracted from inside a grain to the $\Sigma 3(111)$ GB in W, with and without zero-point energy correction. The trapping process is in a sequential manner.

GB in W. More importantly, the H induced GB sliding demonstrated here is a strong support of the H enhanced local plasticity (HELP) mechanism of H embrittlement [24].

To understand more deeply how the multiple H atoms affect the GB properties, we now resort to the change of GB volume. However, for a real material, the introduced H could produce stress to expand the GB core; meanwhile, the bulk part could also hinder the GB to expand freely with lattice deformation. Thus, after implanting H, the material is in the intermediate state between fully relaxed and c axis fixed systems. In order to make clear the

difference between the two kinds of systems, we checked the fully relaxed 6H system and found that its free energy was reduced by 0.53 eV and c axis was extended by 0.77 Å after releasing the force (1.41 eV/Å) on the outermost free surface. Hydrogen could be treated as an incompressible sphere to insert into a cavity (GB core) using the “ball-in-hole” model in continuum elasticity. The elastic energy is about 0.54 eV ($\frac{1}{2} \times 1.41 \times 0.77$), nearly the same as the above mentioned energy release. During this process, the system only release some stored elastic energy and it could be smaller with fewer H implanted into the GB. Here, we only analyze the c axis fixed systems and take the area surrounded by GB(4) and GB(−4) as the GB zone. The first three H atoms induced very small GB volume expansions, which are 0.68, 0.59 and 0.60 Å^3 , respectively. These H atoms have only consumed up the original GB volume. After that, the deformation of the GB structure by implanted H atoms is apparent due to the lack of free volume. The fourth H by inducing a small sliding actually produced a 2.54 Å^3 volume expansion of the GB zone, equivalent to the sum of the previous. Not only did these H atoms act as a barrier to truncate the W–W bonds between the top and bottom parts, but they also compressed the volume of the two parts, making them easily to slide as a closer-packed configuration. The following H could then damage the GB configuration more seriously and cause embrittlement.

Rice Wang thermodynamic theory [25] is appropriate to describe the mechanism of impurity-induced embrittlement by the competition between dislocation crack blunting and brittle boundary separation. The potency of a segregation impurity in reducing the Griffith energy of a brittle boundary separation is a linear function of the difference in binding energies for that impurity at the GB and the free surface [26,27]. To assess the effect of H accumulation at the GB on the decohesion across the boundary plane, we need to investigate the adsorption of H on W (111) surface, which is the eventual state of blistering or cleavage. Our DFT calculations show that totally three H atoms can be adsorbed within the (1×1) unit cell: the first two H atoms are symmetrically aligned along $[110]$; the third one breaks the symmetry slightly and occupy the former two vertical center line, finally each other keeping a distance in the region of $[2.1, 2.3] \text{ Å}$. The binding energies are -1.63 , -1.43 , and -1.29 eV respectively, again in reference to the interstitial H in W bulk. Corrected with ZPE, they become -1.72 , -1.51 , and -1.36 eV . In the absence of H, the cleavage energy of W along a $\Sigma 3(111)$ GB is calculated to be 5.30 eV. With six H segregated, the final state will be three H on each (111) surface. Now, the cleavage energy is as small as 1.06 eV. This means that with a high density of trapped H, the cleavage along $\Sigma 3(111)$ GB in W could become much easier. It is noteworthy that since the seventh H has virtually already broken the GB, more H atoms can segregate to the crack. Therefore the cleavage along the boundary could become even exothermic. A spontaneous formation of H blistering will then follow.

Using the same model [28] as employed in Ref. [14], we can estimate that at room temperature, three H can be trapped the GB and the GB decohesion is as strong as 3.58 eV. At high temperature, even fewer H can be trapped and the GB decohesion as well as the chance for H blistering will be reduced.

We note that with the model adopted here, it is not well defined for the internal stress induced by the H accumulation at the GB in a precise manner. However the atomic compressive stress imposed on the top and bottom layers of the slab have been readily obtained. It is found that with only five H trapped at the GB, the stress on the surface layer of the slab has already attained 10 GPa, which is believed to the magnitude needed for dislocation loop punching. Therefore, we might expect that accumulation of H at the GB is likely, to say the least, to punch dislocation loops in W.

Next, we have performed a similar investigation on an infinitely large dislocation loop in the (001) plane in W (see Fig. 1b).

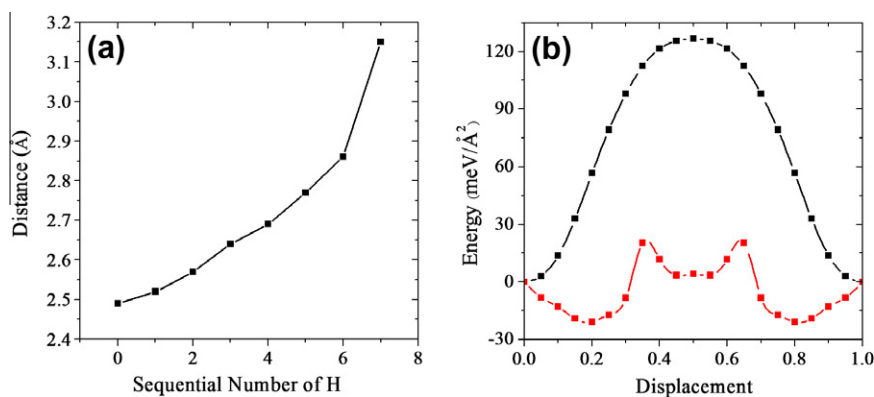


Fig. 4. (a) The distance between GB(2) and GB(-2) W atoms (see Fig. 1 for explanation) as H atom is attracted from inside a grain to the $\Sigma 3(111)$ GB in W. (b) The γ -energy of the $\Sigma 3(111)$ GB of W along $[110]$. The unit of the displacement is the Burgers vector, which is 4.48 \AA . Black and red lines indicate the GB system without H and with seven H impurities respectively. (For interpretation of the references to colour in this figure legend, the reader is referred to the web version of this article.)

Although the border of a dislocation loop cannot be counted by this model, the H-trapping capacity can be estimated reasonably to a large extent. As we did above, we optimized the c axis of the supercell before adding H atoms one by one into the defect. The sequence of H introduction is depicted in Fig. 5. The first H atom was located at the distorted octahedral site, exactly in the plane of the missing atomic layer. The second one then occupied another octahedral site in the neighboring facet. The trapping energies of these two H atoms here is approximately equivalent to those on a (100) free surface. The third and fourth H went to a distorted octahedral site of the top and bottom facet. Upon introducing a fifth one, all these H atoms made a transform to occupy neighboring tetrahedral sites. At last, six H atoms occupied six facets, respectively. Our exhaustive search shows that totally six H atoms can be trapped in each square a^2 (a is the lattice constant) of this dislocation loop. Again, our DFT calculations demonstrated

unambiguously that no H_2 molecules are formed. The calculated trapping energy for each H is shown in Fig. 6. The feature shown here is very similar to the case of H trapping by substitutional He [16] or a mono-vacancy [12–15], as the underlying physics is very similar.

To assess the effect of H accumulation at the dislocation loop on the decohesion across the loop, we have investigated the adsorption of H on W (100) free surface, which is the eventual state after fracture. We find that only two H atoms can be absorbed symmetrically on the bridge of two W atoms on the (100) surface within the (1×1) unit cell. The distance between the two is 2.2 \AA and the binding energies are 1.74 and 1.76 eV , in reference to a H in the perfect bulk. Corrected with ZPE, the trapping energies both become -1.83 eV . With six H segregated, the final state of cleavage will be two H on each (100) surface and one H_2 molecules per (1×1) unit cell. Now, the cleavage energy is reduced from 1.80 eV in the absence of H to -1.96 eV with the help of H atoms. Actually, with four H segregated at high temperature, it could still be reduced to -0.60 eV . This means that with a high density of trapped H, the fracture along (100) dislocation loop could become strongly exothermic.

In all, there is no doubt that the formation of H_2 molecules could occur as long as the vacancy cluster is large enough. However, it is also important to recognize that H_2 molecules cannot form in a single vacancy, grain boundary, and dislocation loop unless additional vacancies are present or micro-cracks form along these defects. This has much to do with the sequence of the formation of micro-cracks and H_2 molecules. Our calculations thus demonstrate

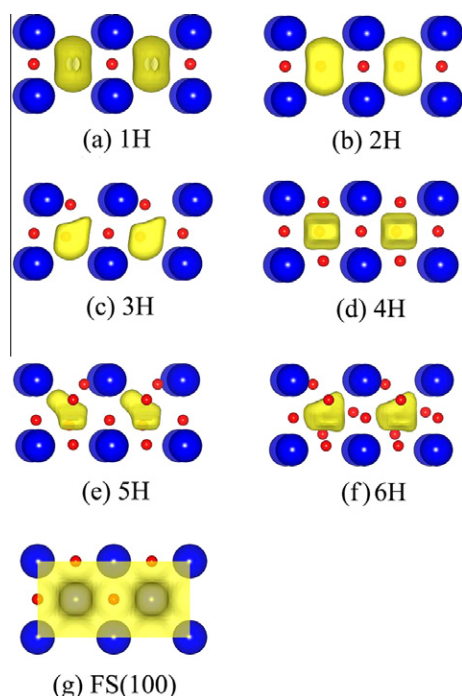


Fig. 5. The calculated geometry and isosurfaces of charge density at a dislocation loop in the (100) plane [subfigures (a)–(f)] and the (100) free surface [subfigure (g)]. Large and blue are W, small and red are H. Yellow curves stand for the charge density isosurfaces of 0.02 e au^{-3} .

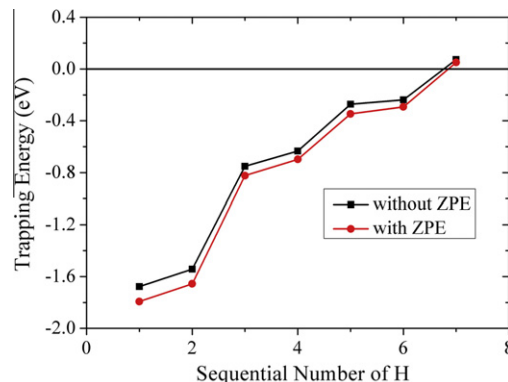


Fig. 6. The calculated trapping energy when one H atom is attracted from a perfect W bulk environment to the inside of a dislocation loop, with and without zero-point energy correction. The trapping process is in a sequential manner.

that the appearance of vacancy clusters is not a necessary condition to initiate hydrogen bubbles.

4. Conclusion

In conclusion, our density functional theory calculations on H trapping at the $\Sigma 3(111)$ tilt grain boundary and dislocation loop in (100) plane indicate that both of the extended defects can trap high density of H atoms. The trapped H weakens severely the cohesion across the boundary or loop plane and can therefore serve as precursors of H blistering. We observe no H_2 molecules are formed, supporting the speculation from experimentalist that the appearance of molecules is related to the formation of voids [29]. Furthermore, a comparison of decohesion effect introduced by H on the grain boundary and dislocation loop in W points to the relevance of free volume associated with defects. The larger the free volume, the stronger the embrittling effect of trapped H, and hence the more compelling force to drive blistering. As a consequence, one strategy to combat H blistering in metals could be reducing the free volume at grain boundaries by introducing segregants with small atomic size. For W, candidates might include Be, B, C, N, and O.

Acknowledgments

The work was supported by the NSFC (Grant No. 50971029), NSFC-ANR (Grant No. 51061130558) and MOST (Grant No. 2011GB108002) of China. The calculations were performed on the Quantum Materials Simulator of USTB.

References

- [1] R.A. Causey, T.J. Venhaus, *Phys. Scripta* T94 (2001) 9.
- [2] R.A. Causey, *J. Nucl. Mater.* 300 (2002) 91.
- [3] C.H. Skinner, A.A. Haasz, V.K. Alimov, N. Bekris, R.A. Causey, R.E.H. Clark, J.P. Coad, J.W. Davis, R.P. Doerner, M. Mayer, A. Pisarev, J. Roth, T. Tanabe, *Fusion Sci. Technol.* 54 (2008) 891.
- [4] M.Y. Ye, H. Kanehara, S. Fukuta, N. Ohno, S. Takamura, *J. Nucl. Mater.* 313–316 (2003) 72.
- [5] V.K. Alimov, J. Roth, R.A. Causey, D.A. Komarov, C. Linsmeier, A. Wiltner, F. Kost, S. Lindig, *J. Nucl. Mater.* 375 (2008) 192.
- [6] K. Tokunaga, M.J. Baldwin, R.P. Doerner, N. Noda, Y. Kubota, N. Yoshida, T. Sogabe, T. Kato, B. Schedler, *J. Nucl. Mater.* 337–339 (2005) 887.
- [7] P. Franzen, C. Garcia-Rosales, H. Plank, V.Kh. Alimov, *J. Nucl. Mater.* 241–243 (1997) 1082.
- [8] W. Xiao, *J. Nucl. Mater.* 421 (2012) 176.
- [9] F.C. Sze, R.P. Doerner, S. Luckhardt, *J. Nucl. Mater.* 264 (1999) 89.
- [10] A.A. Haasz, M. Poon, J.W. Davis, *J. Nucl. Mater.* 266–269 (1999) 520.
- [11] S.M. Myers, M.I. Baskes, H.K. Birnbaum, J.W. Corbett, G.G. Deleo, S.K. Estreicher, E.E. Haller, P. Jena, N.M. Johnson, R. Kirchheim, S.J. Pearton, M.J. Stavola, *Rev. Mod. Phys.* 64 (1992) 559.
- [12] Y.L. Liu, Y. Zhang, H.B. Zhou, G.H. Lu, F. Liu, G.N. Luo, *Phys. Rev. B* 79 (2009) 172103.
- [13] K. Ohsawa, J. Goto, M. Yamakami, M. Yamaguchi, M. Yagi, *Phys. Rev. B* 82 (2010) 184117.
- [14] K. Heinola, T. Ahlgren, K. Nordlund, J. Keinonen, *Phys. Rev. B* 82 (2010) 094102.
- [15] D.F. Johnson, E.A. Carter, *J. Mater. Res.* 25 (2010) 315.
- [16] B. Jiang, F.R. Wan, W.T. Geng, *Phys. Rev. B* 83 (2010) 134112 [In this paper, which was published before Ref. [13] was submitted, it was reported that a monovacancy can trap up to 12 H atoms. Since the focus in this work is on the He–H interaction, details on the trapping of H to a vacancy was not reported.].
- [17] H.B. Zhou, Y.L. Liu, S. Jin, Y. Zhang, G.N. Luo, G.H. Lu, *Nucl. Fusion* 50 (2010) 025016.
- [18] M.J. Attardo, J.M. Galligan, *Acta Metall.* 15 (1967) 395.
- [19] D. Fuks, K. Mundim, V. Liubich, S. Dorfman, *Surf. Rev. Lett.* 6 (1999) 705.
- [20] G. Kresse, J. Furthmüller, *Phys. Rev. B* 54 (1996) 11169.
- [21] P.E. Blochl, *Phys. Rev. B* 50 (1994) 17953.
- [22] G. Kresse, D. Joubert, *Phys. Rev. B* 59 (1999) 1758.
- [23] J.P. Perdew, K. Burke, M. Ernzerhof, *Phys. Rev. Lett.* 77 (1996) 3865.
- [24] H.K. Birnbaum, P. Sofronis, *Mater. Sci. Eng. A* 176 (1994) 191.
- [25] J.R. Rice, J.S. Wang, *Mater. Sci. Eng. A* 107 (1989) 23.
- [26] W.T. Geng, A.J. Freeman, R. Wu, C.B. Geller, J.E. Reynolds, *Phys. Rev. B* 60 (1999) 7149.
- [27] W.T. Geng, A.J. Freeman, *Phys. Rev. B* 63 (2001) 165415.
- [28] F.C. Tompkins, *Chemisorption of Gases on Metals*, Academic Press, London, 1978.
- [29] V.Kh. Alimov, J. Roth, M. Mayer, *J. Nucl. Mater.* 337 (2005) 619.